Journal of Molecular Liquids 427 (2025) 127328

Contents lists available at ScienceDirect

Journal of Molecular Liquids

journal homepage: www.elsevier.com/locate/molliq

Copolymer vs interpenetrated polymer network microgels: The case of poly(N-isopropylacrylamide) and poly(acrylic acid)

Elena Buratti [a,*,1], Silvia Franco [b,c,1], Giulia Di Gregorio [c,2], Francesca Ripanti [c,3], Valentina Nigro [d], Monica Bertoldo [a], Roberta Angelini [b,c,**], Paolo Postorino [c], Barbara Ruzicka [b,c,**]

[a] Department of Chemical, Pharmaceutical and Agricultural Sciences, University of Ferrara, Via L. Borsari 46, Ferrara, 44121, Italy
[b] Institute for Complex Systems, National Research Council (ISC-CNR), Sede Sapienza, Piazzale Aldo Moro, 5, Rome, 00185, Italy
[c] Physics Department, Sapienza University of Rome, Piazzale Aldo Moro 5, Rome, 00185, Italy
[d] ENEA C.R. Frascati, Nuclear Department, Via Enrico Fermi 45, Frascati (Rome), 00044, Italy

ARTICLE INFO

Keywords:
Microgels
Interpenetrated polymer network
Copolymer
PNIPAM
PAAc

ABSTRACT

Microgels based on poly(N-isopropylacrylamide) (PNIPAM) and poly(acrylic acid) (PAAc) were synthesized following two different procedures: random copolymerization of the two monomers, where a single network P(NIPAM-*co*-AAc) microgel is obtained made of the two repeating units, and polymer interpenetration that provides two separate polymer networks within a single microgel structure (PNIPAM-PAAc IPN). We demonstrate that the synthesis procedure has a profound impact on the resulting microgels as shown by investigating swelling, flow and thermal properties as well as the molecular mechanisms driving the microgel behaviour. To this purpose, a systematic study through Dynamic Light Scattering, Rheology, Calorimetry and Raman spectroscopy has been performed at different temperatures, pH values, and concentrations. The direct comparison between P(NIPAM-*co*-AAc) and IPN microgels at same PAAc content, same temperatures, and pH values shows a reduced or even absent temperature responsiveness of the microgel in the first case and a Volume Phase Transition, with a pH dependent swelling ratio, in the second one. The mutual interference or independence of PNIPAM and PAAc reflects in the different properties of copolymerized or interpenetrated microgels as deeply addressed in this work.

1. Introduction

Polymeric materials responsive to external stimuli have garnered great attention in several scientific and technological applications. Among them, polymers composed of both poly(N-isopropylacrylamide) (PNIPAM) and poly(acrylic acid) (PAAc) have emerged as promising due to their distinctive properties and responsiveness to temperature and pH, respectively [1–8]. This class of polymers is often used to synthesize microgels, nano-micro sized particles of crosslinked polymeric networks, with the ability to undergo dramatic changes in their physical and chemical properties in response to external stimuli. In recent years, microgels have gained great attraction in both theoretical and experimental studies due to their unique properties and boundless potentiality [9–13]. They can be synthesized from various polymers, allowing for a wide range of chemical modifications and functionalizations valuable for customized specific applications [14–17]. Microgel particles can retain large amount of water, similarly to biological tissues, providing good prototypes for drug delivery and tissue engineering [18,19]. Moreover, a variety of bioactive molecules, including proteins, enzymes, and nucleic acids, can be incapsulated within microgels pre-

* Corresponding author.
** Corresponding authors at: Institute for Complex Systems, National Research Council, Piazzale Aldo Moro, 5, Rome, 00185, Italy.
E-mail addresses: elena.buratti@unife.it (E. Buratti), roberta.angelini@cnr.it (R. Angelini), barbara.ruzicka@cnr.it (B. Ruzicka).
[1] These authors contributed equally.
[2] Current address: Fondazione Bruno Kessler (Center on Sustainable Energy), Via Sommarive 18, Trento, 38123, Italy; Physics Department, University of Trento, Via Calepina 14, Trento, 38123, Italy.
[3] Current address: Department of Life and Environmental Sciences, Polytechnic University of Marche, Via Brecce Bianche, Ancona, 60131, Italy.

https://doi.org/10.1016/j.molliq.2025.127328
Received 13 September 2024; Received in revised form 2 January 2025; Accepted 6 March 2025
Available online 10 March 2025

serving their activity for applications in biotechnology and medicine [20–22].

The structure, characteristics, and responsiveness of PNIPAM-PAAc based microgels strongly depend on the synthesis method: the procedure of random copolymerization or the creation of an interpenetrating network has a profound impact on the resulting material's properties and applications. Through a random copolymerization of the two monomers, a single-network P(NIPAM-*co*-AAc) microgel is obtained made of two repeating units (derived from NIPAM and AAc) exhibiting properties dependent on the two monomers ratio. The effective charge density of the copolymer can be controlled by the amount of comonomer, the pH and the ionic strength of the medium [23–26]. Instead, by interpenetrating the PAAc network into the PNIPAM one, the obtained PNIPAM-PAAc IPN microgel system provides independent sensitivity to temperature and pH [1,27,26]. The obtained IPN microgel is characterized by a highly dense core of interpenetrated PNIPAM and PAAc networks, surrounded by a low-density shell mainly populated by PAAc chains [28,29]. The properties of IPN are influenced by the interactions between PNIPAM and PAAc, leading to unique responsiveness and characteristics [30,6,31,32]. Therefore, IPN microgels consist of two separate polymer networks within a single microgel structure, whereas copolymer microgels are formed from a single polymer network with a controlled composition of PNIPAM and PAAc units. Comparing these synthesis methods allows scientists and engineers to harness the specific advantages for various applications [25,33,34] and gain a deeper understanding of the underlying science. Indeed, many behaviours of these systems are well-known. For example, for copolymer microgel is demonstrated that the response to temperature and pH usually decrease with increasing acrylic acid content [35,24,36] and that the rheological behaviour differs based on microgel concentration and pH conditions [37,38].

However, even if P(NIPAM-*co*-AAc) microgels [37,39,40] and PNIPAM-PAAc IPN microgels [30,41,5,29] were individually investigated, a clear and detailed comparison between them, particularly at relatively high AAc content, under the same conditions of temperature, pH and concentration, is still lacking. In this work, we investigate and compare the behaviour of these two different architectures, P(NIPAM-*co*-AAc) copolymer and PNIPAM-PAAc IPN microgels, at the same PAAc content, to provide a complete picture as a function of temperature, pH, and concentration.

In particular, our study compares two microgels synthesized using the same random radical precipitation polymerization method: one through a one-step synthesis (copolymer) and the other through a two-step synthesis (IPN). In this way we have studied the effect of synthesis conditions on the material's properties, particularly how the architecture arising from one or two-step radical polymerization impacts swelling, pH-responsiveness, and rheology. To this purpose, a systematic study of swelling, molecular mechanisms driving the microgel behaviour, thermal and flow properties was performed through i) Dynamic Light Scattering (DLS) to investigate the hydrodynamic radius and the microscopic dynamics, ii) Raman spectroscopy to highlight conformational changes induced by microgel collapse and to understand the microscopic interactions in these complex systems, iii) calorimetry to unveil the thermodynamics mechanisms behind the volume phase transition (VPT), and iv) rheology to assess the flow behaviour of these thermoresponsive microgels. This investigation aims to advance the understanding of these fascinating polymeric systems fostering inspiration for additional researches within the realm of responsive microgels.

2. Experimental

2.1. Materials

N-isopropylacrylamide (NIPAM), N,N'-methylene-bis-acrylamide (BIS), acrylic acid (AAc), sodium dodecyl sulphate (SDS) (98% purity), potassium persulfate (KPS) (98% purity), ammonium persulfate (APS) (98% purity), N,N,N',N'-tetramethylethylenediamine (TEMED) (99% purity), ethylenediaminetetraacetic acid (EDTA), $NaHCO_3$ were purchased from Merck KGaA (Darmstadt, Germany). NIPAM monomer and BIS, used as crosslinker, were recrystallized from hexane and methanol respectively, dried under reduced pressure (0.01 mmHg) at room temperature and stored at 253 K. AAc monomer was purified by distillation (40 mmHg, 337 K) under nitrogen atmosphere in presence of hydroquinone and stored at 253 K. SDS, used as surfactant, KPS and APS, used as initiators, TEMED, a reaction accelerator, EDTA, a chelating agent for purifying dialysis membranes, and $NaHCO_3$, were all used as received. All other solvents were RP grade (Carlo Erba) and were used as received. Ultrapure water (resistivity: 18.2 $M\Omega/cm$ at 298 K) was obtained with Sarium® pro Ultrapure water purification Systems, Sartorius Stedim. A dialysis tubing cellulose membrane, MWCO 14000 Da, (Merck KGaA) was cleaned before use by washing with running distilled water for 3 h, treated at 343 K for 10 min into a solution containing 3.0% $NaHCO_3$ and 0.4% EDTA weight concentration, rinsed in distilled water at 343 K for 10 min, and then in fresh distilled water at room temperature for 2 h.

2.2. P(NIPAM-co-AAc) copolymer microgel synthesis

The synthesis of P(NIPAM-*co*-AAc) copolymer microgels consists of a free radical precipitation polymerization, where the two monomer, namely NIPAM and AAc, are added simultaneously in the reaction feed. The polymerization is carried out in presence of a crosslinker (BIS), in order to obtain one single network where the two monomers are randomly distributed and covalently bonded one to each other. Specifically, 3.718 g of NIPAM (0.137 M), 0.93 mL of AAc (0.054 M), 0.293 g of BIS (7.92 mM) and 0.542 g of surfactant (SDS) (7.83 mM) were solubilized in 230 mL of ultrapure water and transferred into a 250 mL four-necked jacketed reactor equipped with condenser and mechanical stirrer. The solution, heated at 343 K, was deoxygenated by purging with nitrogen for 1 h. Then, 0.161 g of KPS (2.48 mM) dissolved in 10 mL of deoxygenated water were added to the solution, in order to start the radical polymerization, carried out for 4 hours. The resultant copolymer microgel was purified by dialysis against distilled water for two weeks changing water frequently. Through gravimetric measurements, the final weight concentration C_w of P(NIPAM-*co*-AAc) micro-particles was determined $\sim 1.25\%$.

2.3. PNIPAM-PAAc IPN microgel synthesis

Differently from the copolymer synthesis, the IPN microgel synthesis is carried out in two steps, following a sequential polymerization method [1]: in the first step, micro-particles consisting of a single homopolymeric PNIPAM network are prepared through a precipitation polymerization, as described by Pelton et al. [42]; in the second one, in presence of the preformed microgel, the acrylic acid is polymerized inside the particle to create a PAAc network interlaced with the first one. A comparison of the synthesis method for copolymer and IPN microgels is shown in Fig. 1.

For this work, in the PNIPAM synthesis, 3.719 g of NIPAM (0.137 M), 0.069 g of BIS (1.87 mM), and 0.541 g of SDS (7.82 mM) were solubilized in 230 mL of ultrapure water and transferred into a 250 mL four-necked jacketed reactor equipped with condenser and mechanical stirrer. The solution was deoxygenated by purging with nitrogen for 1 h and heated at 343 K. The addiction of 0.160 g of KPS (2.47 mM), dissolved in 10 mL of deoxygenated water, started the polymerization, which was stopped after 5 hours. The resultant PNIPAM microgel was purified by dialysis against distilled water for two weeks. Through gravimetric measurements, the final weight concentration C_w of PNIPAM microgel was determined $\sim 1\%$.

In the second step, 24.443 g of the recovered PNIPAM dispersion ($C_w = 1.06\%$) was diluted with ultrapure water up to a volume of 220

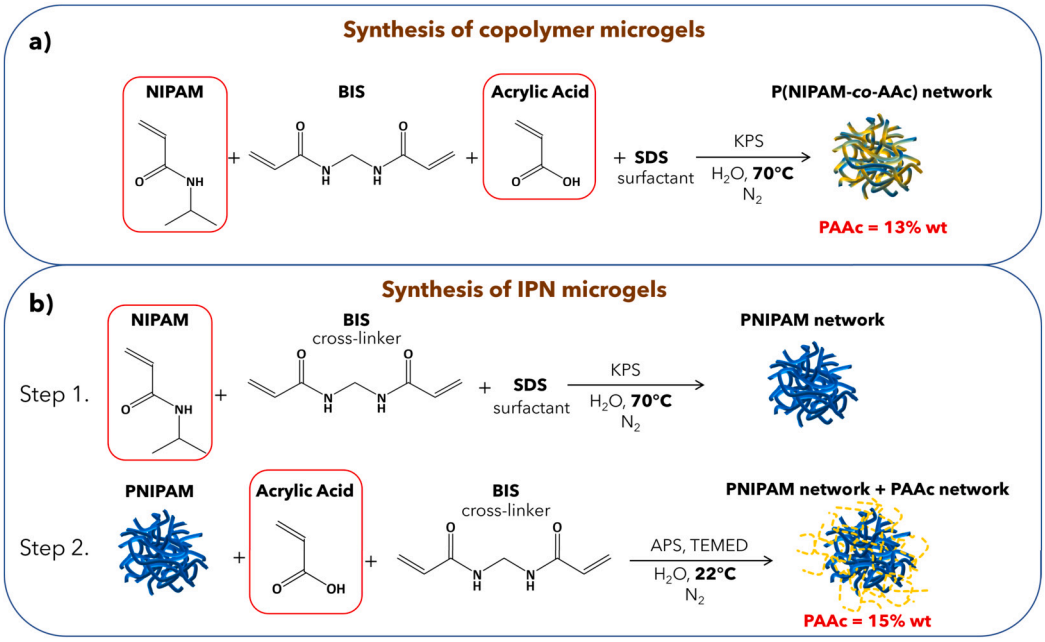

Fig. 1. Scheme of the two different synthesis procedures: a) P(NIPAM-*co*-AAc) copolymer microgel synthesis in one step, the two monomers are added in the same feed reaction to obtain a single network with both the reagents; b) IPN microgel synthesis in two steps and formation of two homopolymeric networks, PNIPAM in blue and PAAc in yellow respectively, interlaced with each other.

mL into a 250 mL four-necked jacketed reactor, kept at 295 K by circulating water. At this temperature, the PNIPAM network is fully swollen and it allows for AAc monomer diffusion into the network, facilitated by hydrogen bonding between the amide groups of PNIPAM and the protonated carboxylic groups of AAc. This mechanism promotes the formation of an interpenetrating polymer network, where the AAc monomer can penetrate both the interior and exterior of the PNIPAM network before polymerization begins. Thus, 0.9 mL of AAc (0.057 M) and 0.195 g of BIS (5.72 mM) were added to the dispersion and the mixture was deoxygenated by bubbling nitrogen inside for 1 h. Then, the polymerization was started with 0.079 g of initiator APS (1.57 mM), adding 0.1 mL of TEMED as accelerator. The reaction, carried on at pH 3, was stopped by exposing to air after 2 h and 15 min. The resultant IPN was purified by dialysing against distilled water with frequent water changes for two weeks, and then lyophilized and redispersed in water to prepare samples at weight concentration C_w = 1.0%.

2.4. Dynamic light scattering

DLS measurements were performed on aqueous suspensions of microgels at different weight concentrations and pH values in a range of temperatures between 293 K and 323 K. Measurements were carried out using an optical setup based on a solid state laser (100 mW) with a monochromatic (λ = 642 nm) and polarized beam, at a scattering angle θ = 90° corresponding to a scattering vector $Q = 0.018\,\mathrm{nm}^{-1}$, according to the relation $Q = (4\pi n/\lambda)\sin(\theta/2)$. The hydrodynamic radius of the particles was obtained through the Stokes-Einstein relation $R_H = k_B T/6\pi\eta D_t$, where k_B is the Boltzmann constant, η the viscosity and D_t the translational diffusion coefficient, related to the relaxation time τ through the relation $\tau = 1/(Q^2 D_t)$. The relaxation time τ was obtained by fitting the autocorrelation function of scattered intensity through the Kohlrausch-William-Watts expression, $g_2(Q,t) = 1 + b[\exp(-(t/\tau)^{\beta})]^2$, as commonly used for colloidal systems with low polydispersity [43], where the stretching exponent β provides the deviation from the single exponential.

The data on the relaxation time as a function of viscosity are well described by an Arrhenius-like functional behaviour for which concentration is used instead of temperature:

$$\tau(C_w) = \tau_0 exp(AC_w) \quad (1)$$

2.5. Raman spectroscopy

Raman measurements were performed by exploiting a Horiba HR-Evolution microspectrometer in backscattering geometry, coupled with a confocal microscope with objectives of different working distances and magnifications. The radiation source is He-Ne laser, λ = 632.8 nm and 30 mW output power (about 15 mW at the sample surface). The setup is equipped with a state-of-the-art optical filtering device based on three BragGrate notch filters, which allow to remove the elastically scattered light and, therefore, to collect Raman spectra at very low frequencies (down to 10 cm^{-1} from the laser line). The detector was a Peltier-cooled charge-coupled device (CCD), with a resolution better than 3 cm^{-1} due to a 600 grooves/mm grating with 800 mm focal length. Measurements reported in this work were performed on aqueous solutions by using quartz cuvettes and were collected with a 20 x objective (0.35 N.A.). Further details on the experimental apparatus can be found in Ref [44]. Measurements have been performed on aqueous suspensions of copolymer and IPN microgels in the temperature range T = 293–313 K across the VPT, at three weight concentrations (C_w = 0.1%, 0.3% and 5.0%) and pH 6.5 and 4.5. Note that several tests have been performed at C_w = 0.1% resulting in long-lasting measurements and a low signal-to-noise ratio.

2.6. Differential scanning calorimetry

Thermal analyses on microgels were performed with a Perkin Elmer Pyris Diamond DSC equipped with Intracooler III as cooling system. About 10-15 mg of microgels dispersions was analysed under nitrogen atmosphere (20 mL/min) in hermetic sealed steel pans (volume of 50 μl), to prevent changes in concentration during the heating/cooling steps. Samples at different concentrations were prepared by pouring a dispersion at 1% into the pans and then evaporating the exceeding solvent in a desiccator, until the desired concentration was reached. The concentration was regularly monitored by accurate weighing of the samples. Once reached the target concentration, pans were hermetically sealed and analysed. The measurements were carried out by cooling the system

from 293 K to 193 K, holding the temperature for 3 min, then heating it to 333 K, holding the temperature for 3 min and finally by cooling it again to 293 K. Each cooling and heating step was carried out with a scanning rate of 5 K/min.

2.7. Rheological measurements

Rheological measurements have been carried out with a rotational rheometer Anton Paar MCR102 with a cone plate geometry (plate diameter = 24.964 mm, cone angle = 1.998°, truncation = 104 μm). Temperature was controlled using a Peltier system and solvent evaporation was avoided thanks to an isolation hood. Before measurements, samples were pre-sheared at shear rate $\gamma = 500\ s^{-1}$ for 30 s in order to erase any mechanical history [25,57] placing them in a reproducible condition. Once loaded, the sample was thermalized for a few minutes before proceeding with the measurement.

Measurements on copolymer and IPN microgels were conducted in rotational mode, varying the stress within an appropriate range as a function of shear rate. Measurements were also performed at a fixed shear rate while varying temperature.

In the case of stress curves as a function of shear rate, data are well described by the Cross model [45–47]:

$$\sigma(\dot{\gamma}) = \dot{\gamma}\left[\eta_\infty + \frac{\eta_0 - \eta_\infty}{1 + (\tau_C\dot{\gamma})^m}\right] \quad (2)$$

where η_0 and η_∞ refer to the viscosities at zero and infinite shear rates, respectively. The parameter m is a power exponent, and τ_C denotes the system's relaxation time, indicating the onset of shear thinning [48]. The inverse of τ_C, $\dot{\gamma}_c$, corresponds to an intermediate critical shear rate. This model is particularly effective for fitting data that display a Newtonian viscosity region at low shear rates, a power-law region at intermediate shear rates, and an infinite viscosity region at high shear rates.

3. Results and discussion

In this work, two microgels with different internal structures, a random copolymer microgel and a IPN microgel, were synthesized, following the procedure reported in Fig. 1. The actual chemical composition of the two systems has been chosen in order to make an effective comparison between the two microgels. It is well known that changing the monomer ratio in the microgels affects the swelling and dynamical behaviours of the particles. In our case, P(NIPAM-*co*-AAc) copolymer and PNIPAM-PAAc IPN microgels with a very similar chemical composition, meaning a similar amount of PAAc in the particles, 13% and 15%, respectively, have been synthesized. The effective composition, obtained through elemental and ^{1}H-NMR analysis, following the procedure explained in a previous work [3], is reported in Table 1. NMR spectra and elemental analysis results can be found in the Supplementary Information (Fig. S1 and Table S1).

3.1. Investigation of microgels swelling behaviour

The swelling behaviour of the synthesized particles with the two different internal structures was investigated by means of Dynamic Light Scattering (DLS) measurements in dilute conditions ($C_w = 0.01\%$), where the particles are non-interacting. The temperature behaviour of their hydrodynamic radii is reported in Fig. 2 in the T = (293÷323) K range, at different pH values between 3.5 and 6.5.

In Fig. 2(a) we compare the single network microgels: the copolymer and the PNIPAM. Copolymer particle radii (R_H = (70÷270) nm at various pH) are always bigger than the PNIPAM one (R_H = 40 nm), even at pH 3.5 where they have their smallest size. This can be explained by the lower SDS/monomers molar ratio in the copolymer reaction feed. The surfactant in the feed was kept at 7.8 mM, just at the SDS critical aggregation concentration (*cac*) (7.8 mM at 343 K, that is the reaction temperature) [49] for both syntheses. However, the monomers amount was different, due to the addition of AAc in the copolymer reaction, leading to a SDS/monomers ratio of 3.94 mol% against the SDS/monomers ratio of 5.63 mol% for the PNIPAM synthesis. Moreover, in addition to the adsorption of surfactant molecules, the particle size during microgel formation is also influenced by the amount of charged fragments that contribute to the surface charge [49]. The higher the number of these charged fragments, the smaller the effect of the adsorbed surfactant molecules on reducing the particle size. This can explain the larger size observed in the copolymer microgel, which is due to the charge contributed by the acrylic acid.

Table 1
Chemical composition of copolymer, PNIPAM and IPN microgel, obtained through elemental and ^{1}H-NMR analysis.

Sample	NIPAM (%)	BIS (%)	AAc (%)
PNIPAM	98.7	1.3	-
IPN	80.3	4.5	15.2
Copolymer	81.1	5.9	13.0

These factors evidently balance the effect of the crosslinking content in these particles: the BIS amount (Table 1) in the copolymer, 5.9 mol%, is higher than the one in PNIPAM microgel, 1.3 mol%, and should lead to smaller particles in the swollen state below the VPT, due to a higher crosslinking degree [50]. However, since the radius values are reversed, this means that we obtained bigger and harder particles in the copolymer and smaller and softer particles in PNIPAM. The lower crosslinker concentration used in the PNIPAM synthesis was intentionally chosen to create a looser network structure. This approach allows for the subsequent incorporation of acrylic acid and the crosslinking of the second network within the first one. Indeed, the initial lower crosslinker concentration in the PNIPAM network facilitates the formation of larger pores, which are essential for the interpenetration and proper integration of the acrylic acid network.

Obviously, another main difference between the PNIPAM and copolymer networks is the presence of a charged monomer, the acrylic acid, in the latter. The particle dimension is clearly affected by the status, protonated or deprotonated, of the carboxylic acid of the AAc. Indeed, when the carboxylic acid is protonated (at pH values below the PAAc pKa, about 4.5), hydrogen bond between other COOH groups or amide groups belonging to the NIPAM units can occur, leading to inter and intra-chain interactions and a shrinking of the network. On the other hand, when the carboxylic acid is deprotonated (at pH values above 4.5), repulsion between these negative charged units, or the negative charge due to the sulfate initiator, happens. In this case, the polymer chains of the network move away from each other and the particle assumes larger dimensions.

The distribution of the charged moieties in the network is crucial to comprehend the microgel behaviour. We can observe this aspect by comparing the copolymer with the interpenetrated structure of the IPN. In the copolymer, the acrylic acid units are mostly inside the network, since AAc reacts faster than NIPAM, similar to the crosslinker kinetic, as we know from the value of the reactivity ratios reported in [51]. However, it is still randomly distributed, since homopolymerization is not fast enough to create a block chain. This means that the copolymer network has a density distribution of the acrylic acid that decreases from the core to the shell, where instead the NIPAM units are predominant. On the contrary, in the IPN particles, the PNIPAM and PAAc networks are formed separately and, from the radii reported in Fig. 2b, we can affirm that the latter network outgrowth the former one during the second step of the synthesis, meaning that in this case the charged moieties are also in the external shell of the particle. As we will show, the different distribution of the acrylic acid in the two systems, and the fact that in one case the two monomers are covalently bonded and in the other one they form two separated networks, affect both the interactions between the chains inside the particle and the interaction between

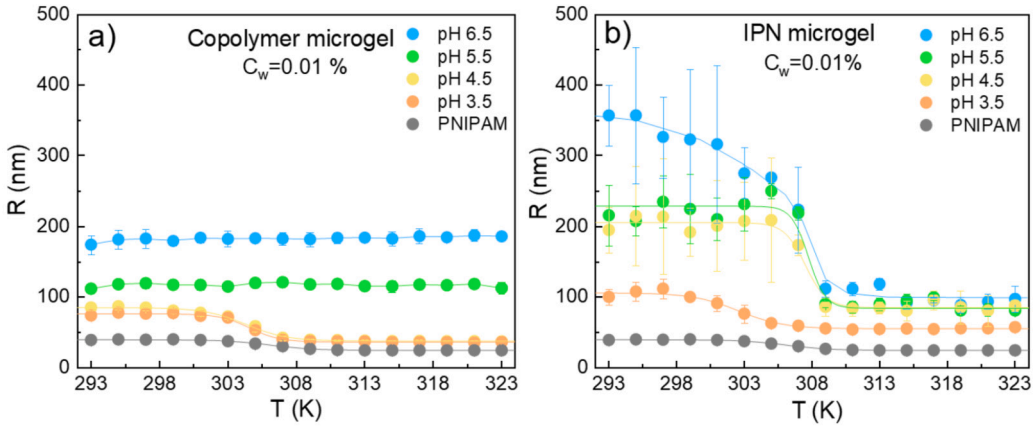

Fig. 2. Hydrodynamic radii of PNIPAM and (**a**) copolymer and (**b**) IPN microgels obtained from DLS measurements as a function of temperature and pH in dilute conditions (C_w = 0.01%). Lines are guides to eyes.

different particles. We also note that polymers made of AAc exhibit a volume phase transition as a function of pH rather than temperature. Specifically, poly(acrylic acid) transition between collapsed and swollen states depends on the ionization state of its carboxylic acid groups. Below a pH of approximately 4.5 (corresponding to the pKa of acrylic acid), PAAc is in a collapsed state because the carboxyl groups (–COOH) are protonated, allowing hydrogen bonding both intra- and intermolecularly. This hydrogen bonding causes aggregation and reduces solubility in water. Above pH 4.5, the carboxylic acid groups become deprotonated ($–COO^-$), creating electrostatic repulsion between negatively charged groups along the polymer chains. This repulsion disrupts the hydrogen bonding and facilitates greater interaction with water molecules, resulting in a swollen, soluble state.

Focusing on the size comparison between the copolymer and the IPN particles (Fig. 2a and 2b, respectively) as a function of temperature and pH, we can initially observe some similarities for the two microgels. Copolymer and IPN show similar radii at low temperature and low pH (about (80÷100) nm), indicating that the similar chemical composition is more effective with respect to the different structure and AAc distribution in the network. Moreover, both samples at low temperature increase the radii by increasing the pH from 3.5 to 6.5. This behaviour is associated to the swelling of the poly(acrylic acid), which is in the dehydrated form at low pH and in the hydrated one above pH 4.5, leading to an increase of the particle size. The fact that the acrylic acid is in the copolymeric or in the interpenetrated configuration does not affect this pH-dependent transition in such conditions of low temperatures. We can also observe that the increase in the particle radius of the IPN as a function of pH is higher than that of the copolymer, reaching values up to 350 nm at pH 6.5. A plausible explanation for this observation could be related to the distribution of the crosslinker within the PAAc network in the IPN. It is likely that the PAAc shell is not highly crosslinked, with most of the crosslinker concentrated within the PNIPAM/PAAc core. This would result in a portion of the PAAc network extending outward as relatively long dangling chains, contributing to the observed increase in particle radius.

A different picture arises increasing temperature. For the copolymer (Fig. 2a) the radius shrinks only at the lowest values of pH (that are 3.5 and 4.5) and it remains constant for higher pH. For IPN microgel (Fig. 2b), it shrinks at all the investigated pH towards very similar values at 323 K. It is evident that for the copolymer the swollen-shrunken transition around 305 K typical of PNIPAM is not present. This pH-affected behaviour of the copolymer microgel was already observed by Farooqi et al. [36] for microgel with a not negligible amount of PAAc (around 9%). This picture is also confirmed from simulations on the effect of the charges content, demonstrating that the VPT is still visible in the copolymer at low AAc content, but it disappears when the concentration of acrylic acid exceeds 5% [52]. This observation is in agreement with our results on copolymer microgel. At variance, IPN microgel preserves a clear VPT at all pH even at 15% PAAc content. In fact, in IPN microgels PAAc is not covalently bonded to the PNIPAM network but two homopolymeric crosslinked independent networks made of PNIPAM and PAAc are formed. On the other hand, since PNIPAM hydration-dehydratation is governed by the interaction between water molecules and the isopropylic moiety [53], it is evident that in the copolymer structure, where the AAc monomer interrupts the PNIPAM chain, the aggregation of the isopropylic groups at increasing of temperature is less favoured. Another distinctive peculiarity of IPN is the effect of the pH in the swelling profile at pH 3.5, where the volume phase transition temperature is shifted towards a lower value with respect to higher pH. This result can be ascribed to the presence of the shrunken PAAc network around the PNIPAM one, creating an hydrophobic environment that leads to an anticipation of the transition. The same hydrophobic environment cannot be created in the random copolymer, thus the transition at pH 3.5 appears at the well-known temperature of the PNIPAM systems.

A consideration on the different structure of copolymer and IPN microgels can be done by observing the stretching parameter β (Fig. 3) related to the polydispersity index [54]. For copolymer microgels, there are no changes with temperature and pH: all β values are around 1, indicating a quite monodispersed colloidal suspension. For IPN microgels, instead, β exhibits values between 0.8 and 0.9, indicating that samples are slightly more polydisperse. However, also in this case β is quite constant with temperature, we can just observe a small increase above the Volume Phase Transition Temperature (VPTT), associated with the contraction of the PNIPAM network in the particles [32]. The behaviour of IPN at pH 4.5 should be noted, since this sample has the lowest β value, down to 0.7: at this pH, that is at the pKa of the acrylic acid, the system is at a protonation-deprotonation equilibrium, where some carboxylic groups of the polyacrylic acid network are protonated while others remain deprotonated. This coexistence of two species (COOH and COO^-) could lead to local heterogeneities in the particle structure, potentially influencing the particle's conformation and contributing to the observed decrease in the value of β. This equilibrium does not occur at pH 3.5, pH 5.5 and 6.5, where the moieties are almost all protonated or not protonated and thus the network is prevalently in the shrunken or in the swollen form, respectively. Comparing the β parameter of copolymer and IPN, it is evident that the lower values for IPN are due to the interpenetrated structure, where PAAc network polymerises outgrowing the PNIPAM particle at variance with the copolymer, that is synthesised in one single step and in presence of a surfactant. In other words, the slightly higher polydispersity of IPN microgel is due to an higher fuzziness of the shell of the particles, which decreases when the network shrunk, as at low pH and high temperatures.

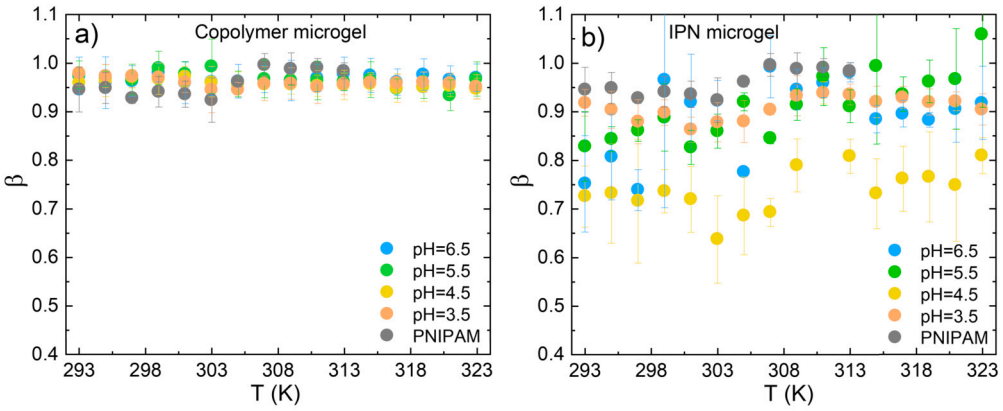

Fig. 3. Stretching parameter β of PNIPAM and (**a**) IPN microgels and (**b**) copolymer obtained from DLS measurements as a function of temperature and pH in dilute conditions ($C_w = 0.01\%$).

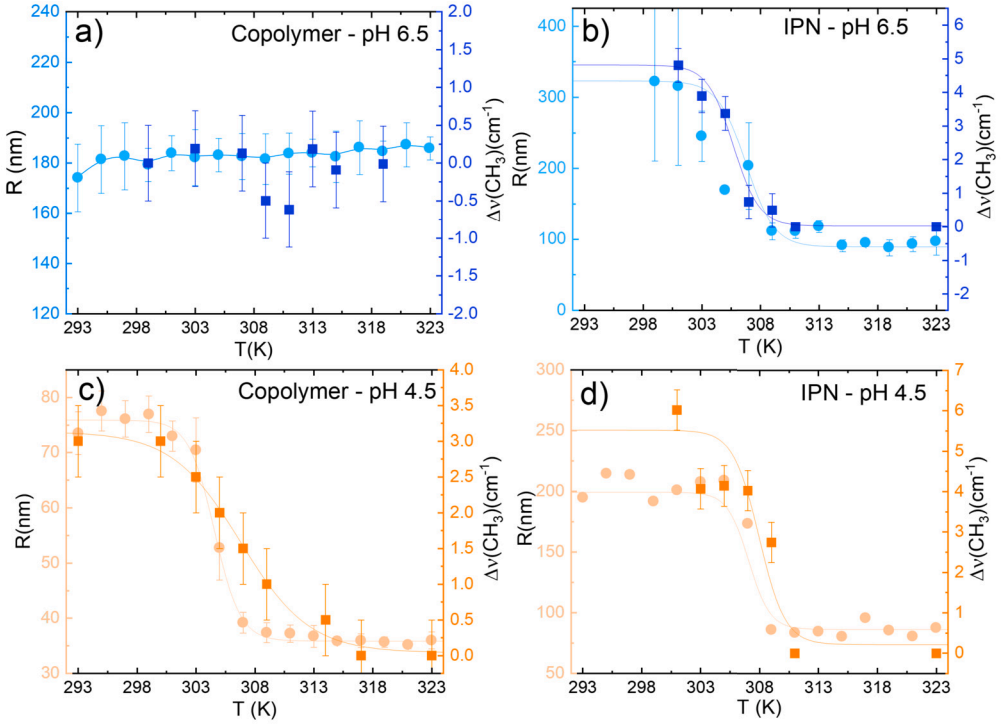

Fig. 4. Hydrodynamic radii R_H (left axis, circles) and antisymmetric CH_3 frequency shift $\Delta\nu$ (right axis, squares) as a function of temperature for copolymer microgel at (**a**) pH 6.5 and (**c**) pH 4.5 and for IPN at (**b**) pH 6.5 and (**d**) pH 4.5.

The swelling behaviour as a function of temperature and pH observed by DLS measurements was confirmed also by Raman spectroscopy. Previous works in literature [55,28] showed that the shrinking of PNIPAM-based microgels across the VPTT involves molecular changes that can be probed by Raman spectroscopy. Therefore, we performed Raman measurements on copolymer and IPN microgels in order to investigate the molecular mechanism that drives the VPT. Both microgels were measured at $C_w = 5.0\%$ at different temperatures across the VPTT and two pH (4.5 and 6.5). Measurements were carried out also at $C_w = 0.01\%$, giving similar results but with a low signal-to-noise ratio. Examples of Raman spectra in the range of interest of copolymer and IPN microgel as a function of temperature are reported in the Supplementary Information (Figs. S2 and S3). We focus our attention on the spectral range between 2825 cm^{-1} and 3025 cm^{-1} that is related to vibrations of the CH_2 and CH_3 groups. Indeed, it has been reported that this spectral region is sensitive to variations in the hydrogen bond due to the different interactions among polymers and between polymer side groups and water molecules surrounding them [28]. For example, it has been demonstrated that the highest number of water molecules surrounding the CH_3 groups correlates with the highest frequency of the antisymmetric CH_3 stretching (peak at 2988 cm^{-1}) [56,57]. Therefore, a shift in frequency of the antisymmetric CH_3 stretching means that the microgel is undergoing a VPT from the swollen hydrated state to the shrunken dehydrated one.

According to a previous work [28], the spectra in this region were deconvoluted by four Gaussian components and the variations of the contribution assigned to the antisymmetric stretching of CH_3 around 2988 cm^{-1} were investigated. Examination of the peak frequency reveals that, by increasing temperature, there is a downshift of the CH_3 antisymmetric mode in almost all the investigated samples. This shift is related to the dehydration of the isopropyl group of NIPAM, suggesting that, when increasing the temperature, the amount of water molecules surrounding the isopropyl group is reduced with a consequent increase of the internal microgel packing density. In particular, Raman and DLS results for copolymer and IPN at pH 4.5 and 6.5 are compared in Fig. 4 where the hydrodynamic radius is reported on the

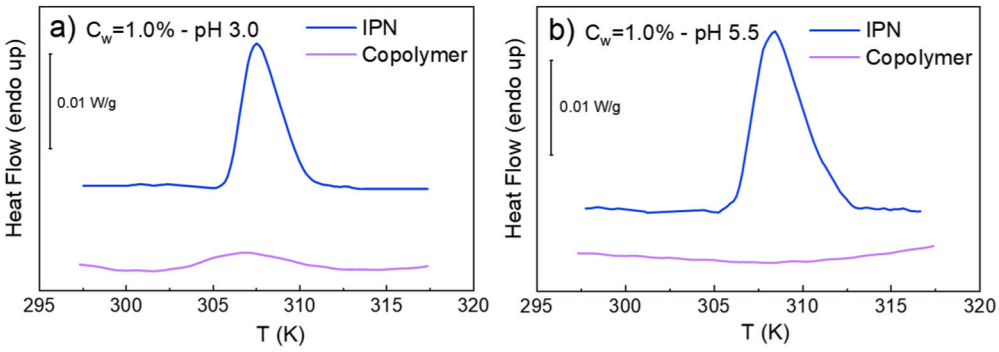

Fig. 5. DSC thermograms for copolymer and IPN microgels at concentration C_w = 0.1% at (**a**) pH 3.0 and (**b**) pH 5.5 at a heating rate 10 K/min. Curves are vertically shifted for clarity.

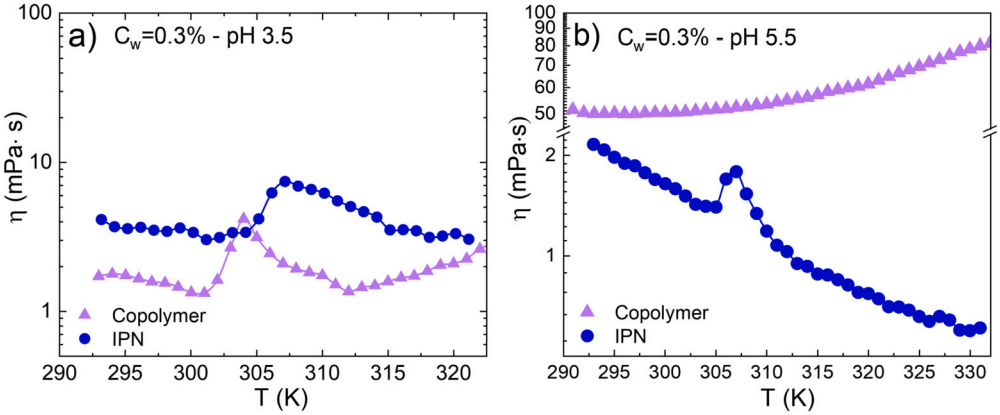

Fig. 6. Viscosity of copolymer and IPN microgels as a function of temperature, at heating rate 0.5 K/min, at concentration C_w = 0.3% at (a) pH 3.5 and (b) pH 5.5.

left axis (circles, light colours) and the peak frequency shift on the right one (squares, dark colours). The hydrodynamic radius and the frequency shift have similar temperature behaviour for all the investigated microgel and pH, demonstrating that Raman spectroscopy is capable to follow the swelling behaviour obtained by DLS analysis. We can observe that in the IPN at pH 4.5 and 6.5 the CH_3 peak frequency abruptly shifts following the typical sharp transition at the VPTT. For the copolymer, the frequency undergoes a volume phase transition only at pH 4.5 and not at pH 6.5, where it is quite constant over all the range of temperatures, in line with the DLS results and confirming that the behaviour is a consequence of the AAc and NIPAM interaction in the copolymer structure, as mentioned above.

The swelling behaviour of copolymer and IPN microgels at both pH was also investigated by calorimetric measurements at heating rate 10 K/min for the samples at C_w = 1.0%. In Fig. 5, the thermograms of IPN microgel at pH 3.0 and pH 5.5, reported in panel (a) and panel (b), respectively, show the expected endothermic peaks around the VPTT, while the thermograms of copolymer microgel show a small peak at pH 3.0 and a flat curve at pH 5.5, confirming no transition in this condition. The onset temperatures, T_{on}, obtained from the analysis of the curves, for the copolymer at pH 3.0 is 303.4 K and for the IPN microgel are 305.9 K and 306.2 K at pH 3.0 and 5.5, respectively, in agreement with a previous work [29], where the VPTT at low pH is lower than the one at pH above the pKa value. The slightly anticipated transition at low pH is due to the insolubility of PAAc in water, with the consequent shrinking of the network, which creates a more hydrophobic environment where NIPAM starts to collapse.

Moreover, at this pH, a complexion between the protonated COOH groups of acrylic acid and the amide group (CONH) of NIPAM occurs, as well explained in Ref [29], affecting the interaction of the microgel with water molecules. This effect can be noted in the values of normalized enthalpy variation, ΔH, that are 0.23 J/g at pH 3.0 and 0.32 J/g at pH 5.5. Since the energy of the transition is related to the dehydration process of the isopropylic groups of PNIPAM, it is evident that at low pH, when some of the NIPAM units are already involved in bonds with acrylic acid moieties and not with water, the dehydration process requires less energy. On the contrary, at high pH the complexation is broken due to the deprotonation of the carboxylic acid moieties and almost all the NIPAM repeating units are involved in the transition, explaining the higher ΔH value. This reasoning can be applied also to explain the quite low enthalpy value of the copolymer at pH 3.0: in this case, the acrylic acid is randomly copolymerised in the network, located prevalently towards the core of the particle and not in the shell, as we mentioned before [51], and all the AAc repeating units are near to the NIPAM ones, interacting efficiently with the amide moieties. Thus, the number of NIPAM repeating units involved in the complexation is higher in the copolymer than in the case of the IPN, where, on the contrary, probably only the AAc inside the particle, and not the ones in the outer shell, can effectively interact with the NIPAM moieties. This means that a lower amount of NIPAM units contribute to the transition in the copolymer, explaining the lower ΔH value with respect to the IPN in the same conditions.

Viscosity measurements as a function of temperature, carried out at pH 3.5 and 5.5 at C_w = 0.3% (Fig. 6), clearly show the VPT for the IPN as expected. Indeed, the increase of viscosity around 305 K and the subsequent decrease appears in correspondence of the shrinking of the microgel. As reported in [58,31] this behaviour can be explained considering that the particles start to collapse exposing a more “sticky” shell, which favours weakly aggregation due to entanglement of chains between different particles. Then the particle cores further collapse, the charge groups locate at the particle surface and the microgels revert to the behaviour of the more familiar state of charge-stabilised latexes in suspension with repulsive charges that prevent aggregation. As mentioned above, this phenomenon, even if proposed for PNIPAM microgels, well describes the IPN behaviour where the charged groups of the PAAc

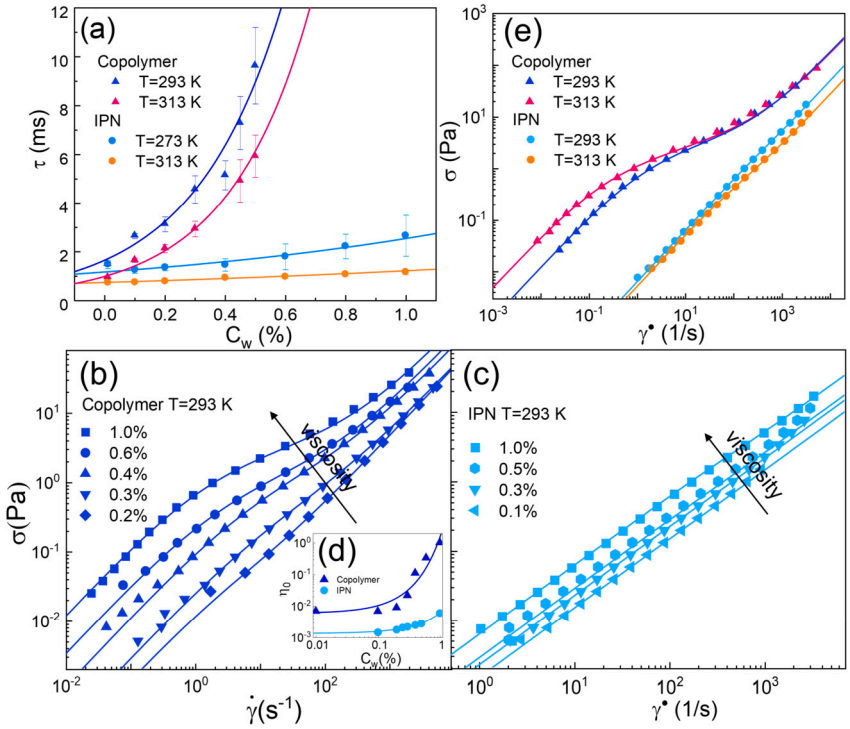

Fig. 7. (**a**) Relaxation times τ as a function of concentration and (**e**) shear stress σ as a function of the shear rate $\dot{\gamma}$ for copolymer and IPN microgel at C_w = 1.0%, pH 5.5 and at T = 293 k and 313 k. Shear stress as a function of the shear rate for (**b**) copolymer and (**c**) IPN microgels at pH 5.5, T = 293 K and at the indicated concentrations. (**d**) Viscosity η_0 as a function of concentration for copolymer and IPN microgels. Relaxation times data were fitted with Arrhenius model. Shear stress data were fitted with a Cross model.

are in the external shell of the particle network. This explanation fits for both pH; in fact, at pH 5.5 the PAAc network is swollen and the chain entanglements due to some weakly interaction can occur, even if most of the AAc moieties are deprotonated; at pH 3.5, the PAAc is protonated and the network is collapsed but still outside the PNIPAM particle, as demonstrated by DLS measurements (Fig. 2), where the diameter of the IPN is higher than the PNIPAM one. For the copolymer, the transition is visible only at pH 3.5 as expected, in agreement with DLS and calorimetric measurements shown respectively in Fig. 2 and Fig. 5(a). As already found above, at pH 5.5, value higher than the PAAc pKa, no transition is found; moreover, we can observe that the viscosity is quite high even at a low concentration as C_w = 0.3%.

3.2. Behaviour at increasing concentration

In order to compare the effect of concentration on microgel properties, a systematic investigation of both systems was conducted at fixed pH of 3.5 and 5.5.

Data obtained at pH 5.5 are shown in Fig. 7, in particular in Fig. 7(a) the relaxation time τ obtained from DLS measurements for copolymer and IPN microgels at temperature below (293 K) and above (313 K) the VPTT are reported as a function of concentration C_w. For both microgels the relaxation time increases by increasing the concentration of particles, suggesting a slowing down of the dynamics, related to an aggregation of the particles at higher concentrations, due to interparticles interactions [32,29]. We can also observe a very different behaviour for the copolymer: the relaxation time shows a steeper exponential increase with respect to IPN, reaching the maximum measurable value at C_w = 0.5%. From this result, we can assume that, at concentrations C_w > 0.5%, the system passes from a fluid phase to an arrested state undergoing an ergodic to non-ergodic transition. Data are fitted with the Arrhenius model $\tau(C_w) = \tau_0 exp(AC_w)$ and the glass transition concentrations, C_g, (defined as the concentration where τ = 100 s) are C_g = (3.2 ± 0.6) % at 293 K and C_g = (3.1 ± 0.4) % at 313 K. For the IPN, the relaxation time is measurable up to C_w = 1.0% and also in this case data can be fitted with an Arrhenius equation providing C_g higher than 14% at both temperatures. Thus, at the highest measured concentration, C_w = 1.0%, the sample is far from being arrested, probably due to the exposed network of PAAc in the structure that, at pH 5.5, presents deprotonated carboxylic acids moieties that prevent particles aggregation due to repulsive interactions.

Rheological measurements as a function of concentration, up to C_w = 1.0%, highlight the differences between the two classes of microgels. Fig. 7(b) presents the shear stress σ as a function of shear rate $\dot{\gamma}$ at T = 293 K for copolymeric microgels within the weight concentration range of (0.1–1.0)%. At low concentrations, the flow curves exhibit an almost Newtonian behaviour ($\sigma \propto \dot{\gamma}$), whereas at higher concentrations, they progressively deviate toward a shear-thinning regime. In contrast, the flow curves of IPN microgels, shown in Fig. 7(c), maintain the characteristics of low-viscosity liquids across the entire investigated concentration range, displaying a nearly Newtonian behaviour throughout. All data were analyzed using the Cross model, as described by Equation (2). The parameter η_0 representing zero-shear viscosity, as a function of concentration is reported in Fig. 7(d). The observed increase in viscosity with concentration reflects the slowing down of particle dynamics, with two distinct trends: a steeper rise in viscosity for copolymeric microgels, consistent with the relaxation time results. These rheological findings are better summarized in Fig. 7(e) where the shear stress σ as a function of the shear rate $\dot{\gamma}$ for both microgels at 293 K and 313 K is reported. For IPN, the shear stress is quite linear with the shear rate, indicating an almost Newtonian behaviour and thus a liquid state both at 293 K and 313 K. The copolymer instead shows a shear-thinning behaviour at both temperatures, with higher stress values, confirming the more viscous nature of this sample. This behaviour precursor of an yield stress is typical of a system going towards an arrested state, as also demonstrated in [31]. It should be noted that increasing temperature the transition towards an arrested state is favoured, as evident from the higher stress value for the sample at higher temperature.

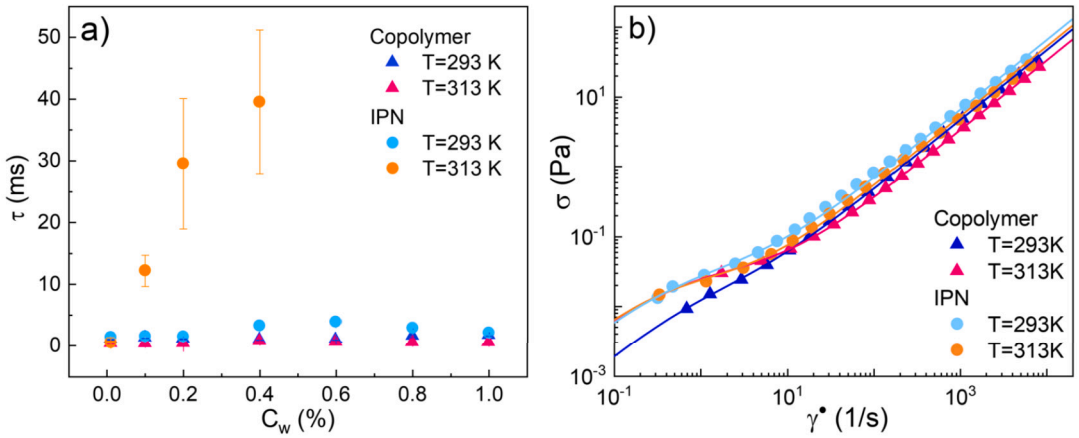

Fig. 8. a) Relaxation times τ as a function of concentration C_w and **b**) shear stress σ as a function of the shear rate $\dot{\gamma}$ for copolymer and IPN microgel at pH 3.5 and at T = 293 K and 313 K. Shear stress data were collected at C_w = 1.0% and fitted with the Cross model.

Data obtained at pH 3.5, where the PAAc is in the shrunken state, are shown in Fig. 8. The relaxation time, reported in Fig. 8(a), for IPN and copolymer show a different behaviour in concentration with respect to those obtained at pH 5.5: for copolymer microgels, τ is quite small and constant at both 293 K and 313 K, indicating a liquid phase up to C_w = 1.0%; for IPN microgels, data at 293 K are similar to the copolymer ones but at 313 K they exponentially increase in the concentration range (0.01÷0.4) %, above which samples are no longer measurable. This means that IPN at low pH and high temperature aggregates at very low concentration, due to hydrogen-bond interactions between the protonated carboxylic acid in the outer shell of different particles. Moreover, the negative charge belonging to the PNIPAM network due to the KPS initiator is mostly inside the particle, covered by the collapsed PAAc network, thus the repulsion that stabilize the colloidal dispersion is no longer happening. We should note that, instead, in the copolymer the negative charged moieties of PNIPAM are still outside the network, while the protonated ones of PAAc are inside, not able to bond with other protonated moieties of other particles, thus the repulsion is still maintained. The aggregation of IPN particles does not happen at low temperature because the PAAc network is shrunken but the PNIPAM one is swollen, inhibiting the interaction between the COOH moieties. On the contrary, at high temperature both networks are collapsed, exposing the PAAc that is in the "hydrophobic" condition, leading to an aggregation of particles.

Viscosity measurements as a function of shear rate at C_w = 1.0% show a similar behaviour between copolymer and IPN microgels at 293 K and 313 K, with a slight increase of stress for IPN at very low shear rates, as shown in Fig. 8(b), where the shear stress $\sigma(\dot{\gamma})$ is reported. For copolymer microgels, the shear stress is quite linear with the shear rate, indicating an almost Newtonian behaviour and thus a liquid state both below and above the VPTT. On the other hand, IPN microgels show slightly higher stress values, indicating a more viscous nature of samples. It should be noted that, at variance with pH 5.5, the transition towards yield stress behaviour is less evident independently from temperature. Moreover, at variance with the structural relaxation time behaviour at T = 313 K (Fig. 8(a)), the stress curve obtained from rheology does not manifest the yield stress typical of an arrested state. This can be explained considering that, although particles form aggregates (increase of τ), they could not give rise to a macroscopic arrested state.

4. Conclusions

In conclusion, through DLS, Raman, calorimetric and rheological measurements on copolymer and interpenetrated polymer network microgels with same chemical composition, we have shown how the different internal structure affects their behaviour.

In the case of P(NIPAM-*co*-AAc) microgels, the incorporation of carboxylic acid groups of AAc produces a significant mutual interference with PNIPAM, resulting in a reduced or even absent temperature responsiveness of the microgel at increasing pH. On the contrary, interpenetration of the PAAc and PNIPAM networks provides, at least at these investigated PAAc content, independent sensitivity to temperature and pH, preserving the same Volume Phase Transition of pure PNIPAM microgel. This is evident from the comparison between the hydrodynamic radii and antisimmetric CH_3 frequency shifts for copolymer and IPN microgels at low and high pH shown in Fig. 4. The same behaviour is found from calorimetric and rheology measurements.

A different behaviour between the two systems is also found at increasing concentrations. In particular, at pH 5.5 both microgels show the slowing down of the dynamics typical of aggregating samples. In the case of P(NIPAM-*co*-AAc) microgels, the interactions between particles must be more effective, since the divergence of the relaxation time happens at lower concentrations with respect to IPN microgels and rheological measurements evidence a behaviour precursor of yield stress typical systems approaching an arrested state. In the case of pH 3.0, DLS and rheological data do not show any significant evidence of formation of arrested states. Moreover, DLS measurements indicate that at low pH and high temperature aggregates at very low concentration, probably due to hydrogen-bond interactions between the protonated carboxylic acid in the outer shell of different particles, must be formed (divergence of the relaxation time). However, these aggregates do not give rise to a macroscopic arrested state as evident from the stress curves that do not show any yield stress typical of an arrested state.

CRediT authorship contribution statement

Elena Buratti: Writing – review & editing, Writing – original draft, Visualization, Methodology, Investigation, Formal analysis, Data curation, Conceptualization. **Silvia Franco:** Writing – review & editing, Writing – original draft, Visualization, Methodology, Investigation, Formal analysis, Data curation, Conceptualization. **Giulia Di Gregorio:** Investigation, Formal analysis, Data curation. **Francesca Ripanti:** Writing – review & editing, Methodology, Data curation. **Valentina Nigro:** Writing – review & editing, Validation. **Monica Bertoldo:** Writing – review & editing, Validation. **Roberta Angelini:** Writing – review & editing, Validation, Supervision, Resources, Project administration, Funding acquisition, Conceptualization. **Paolo Postorino:** Writing – review & editing, Validation, Supervision, Resources, Project administration, Funding acquisition. **Barbara Ruzicka:** Writing – review & editing, Validation, Supervision, Resources, Project administration, Funding acquisition, Conceptualization.

Declaration of competing interest

The authors declare that they have no known competing financial interests or personal relationships that could have appeared to influence the work reported in this paper.

Acknowledgements

RA, SF and BR acknowledge the Project ECS 0000024 Rome Technopole, – CUP B83C22002890005, NRRP Mission 4 Component 2 Investment 1.5, funded by the European Union – NextGenerationEU. RA acknowledges financial support under the National Recovery and Resilience Plan (NRRP), Mission 4, Component 2, Investment 1.1, Call for tender No. 104 published on 2.2.2022 by the Italian Ministry of University and Research (MUR), funded by the European Union – NextGenerationEU – Project PRIN 2022ZA77J2 ICARUS – CUP B53D23009010006.

Appendix A. Supplementary material

Supplementary material related to this article can be found online at https://doi.org/10.1016/j.molliq.2025.127328.

Data availability

Data will be made available on request.

References

[1] X. Xia, Z. Hu, Synthesis and light scattering study of microgels with interpenetrating polymer networks, Langmuir 20 (2004) 2094–2098.
[2] J. Mattsson, H.M. Wyss, A. Fernandez-Nieves, K. Miyazaki, Z. Hu, D. Reichman, D.A. Weitz, Soft colloids make strong glasses, Nature 462 (5) (2009) 83–86.
[3] N. Micali, M. Bertoldo, E. Buratti, V. Nigro, R. Angelini, V. Villari, Interpenetrating polymer network microgels in water: effect of composition on the structural properties and electrosteric interactions, ChemPhysChem 19 (2018) 2894–2901.
[4] V.Y. Grinberg, T.V. Burova, N.V. Grinberg, A.G. Buyanovskaya, A.R. Khokhlov, E.Y. Kozhunova, O.V. Vyshivannaya, I.R. Nasimova, Functionalized thermoresponsive microgels based on n-isopropylacrylamide: energetics and mechanism of phase transitions, Eur. Polym. J. 133 (2020) 109722.
[5] V. Nigro, R. Angelini, M. Bertoldo, E. Buratti, S. Franco, B. Ruzicka, Chemical-physical behaviour of microgels made of interpenetrating polymer networks of PNIPAM and poly(acrylic acid), Polymers 13 (2021) 1353–1378.
[6] S. Franco, E. Buratti, B. Ruzicka, V. Nigro, N. Zoratto, P. Matricardi, E. Zaccarelli, R. Angelini, Volume fraction determination of microgel composed of interpenetrating polymer networks of PNIPAM and polyacrylic acid, J. Phys. Condens. Matter 33 (17) (2021) 174004.
[7] G.A. Komarova, R.A. Gumerov, V.Y. Rudyak, E.Y. Kozhunova, I.I. Potemkin, I.R. Nasimova, Peculiarities of emulsions stabilized by stimuli-responsive interpenetrating polymeric network microgels, Langmuir 40 (18) (2024) 9414–9425.
[8] S. Franco, B. Ruzicka, R. Angelini, Soft and responsive: rheological insights into PNIPAM based microgels and applications, J. Phys. Condens. Matter (2025), https://doi.org/10.1088/1361-648X/adbb9a.
[9] T. Hoare, R. Pelton, Functionalized microgel swelling: comparing theory and experiment, J. Phys. Chem. B 111 (41) (2007) 11895–11906.
[10] E. Buratti, I. Sanzari, F. Dinelli, T. Prodromakis, M. Bertoldo, Formation and stability of smooth thin films with soft microgels made of poly (n-isopropylacrylamide) and poly (acrylic acid), Polymers 12 (11) (2020) 2638.
[11] N. Hazra, A. Ninarello, A. Scotti, J.E. Houston, P. Mota-Santiago, E. Zaccarelli, J.J. Crassous, Structure of responsive microgels down to ultralow cross-linkings, Macromolecules 57 (1) (2023) 339–355.
[12] V. Nigro, E. Buratti, F. Limosani, R. Angelini, F. Dinelli, S. Franco, E. Nichelatti, M. Piccinini, M.A. Vincenti, R.M. Montereali, et al., Spin-coating deposition of thermoresponsive microgel thin films, Colloids Surf. A, Physicochem. Eng. Asp. 674 (2023) 131918.
[13] S. Franco, L. Severini, E. Buratti, L. Tavagnacco, S. Sennato, L. Micheli, M. Missori, B. Ruzicka, C. Mazzuca, E. Zaccarelli, R. Angelini, Gellan-based hydrogels and microgels: a rheological perspective, Carbohydr. Polym. 354 (2025) 123329.
[14] T. Hoare, R. Pelton, Highly ph and temperature responsive microgels functionalized with vinylacetic acid, Macromolecules 37 (7) (2004) 2544–2550.
[15] T. Hoare, R. Pelton, Electrophoresis of functionalized microgels: morphological insights, Polymer 46 (4) (2005) 1139–1150.
[16] V. Sáez-Martínez, L. Pérez-Álvarez, M. Merrero, E. Hernáez, I. Katime, pH-sensitive microgels functionalized with folic acid, Eur. Polym. J. 44 (5) (2008) 1309–1322.
[17] T. Hoare, R. Pelton, Impact of microgel morphology on functionalized microgel- drug interactions, Langmuir 24 (3) (2008) 1005–1012.
[18] S.V. Vinogradov, Colloidal microgels in drug delivery applications, Curr. Pharm. Des. 12 (2006) 4703–4712.
[19] Q. Feng, D. Li, Q. Li, X. Cao, H. Dong, Microgel assembly: fabrication, characteristics and application in tissue engineering and regenerative medicine, Bioact. Mater. 9 (2022) 105–119.
[20] Y. Zhang, W. Zhu, B. Wang, J. Ding, A novel microgel and associated post-fabrication encapsulation technique of proteins, J. Control. Release 105 (3) (2005) 260–268.
[21] N.M. Smeets, T. Hoare, Designing responsive microgels for drug delivery applications, J. Polym. Sci., Part A, Polym. Chem. 51 (14) (2013) 3027–3043.
[22] A.S. Caldwell, G.T. Campbell, K.M. Shekiro, K.S. Anseth, Clickable microgel scaffolds as platforms for 3d cell encapsulation, Adv. Healthc. Mater. 6 (15) (2017) 1700254.
[23] M.J. Snowden, B.Z. Chowdhry, B. Vincentb, G.E. Morris, Colloidal copolymer microgels of N-isopropylacrylamide and acrylic acid: pH, ionic strength and temperature effects, J. Chem. Soc. Faraday Trans. 92 (1996) 5013–5016.
[24] K. Kratz, T. Hellweg, W. Eimer, Influence of charge density on the swelling of colloidal poly(N-isopropylacrylamide-co-acrylic acid) microgels, Colloids Surf. A, Physicochem. Eng. Asp. 170 (2000) 137–149.
[25] S. Schmidt, T. Hellweg, R. von Klitzing, Packing density control in p (nipam-co-aac) microgel monolayers: effect of surface charge, ph, and preparation technique, Langmuir 24 (21) (2008) 12595–12602.
[26] R. Begum, Z.H. Farooqi, S.R. Khan, Poly (n-isopropylacrylamide-acrylic acid) copolymer microgels for various applications: a review, Int. J. Polym. Mater. Polym. Biomater. 65 (16) (2016) 841–852.
[27] J. Ma, B. Fan, B. Liang, J. Xu, Synthesis and characterization of poly (n-isopropylacrylamide)/poly (acrylic acid) semi-ipn nanocomposite microgels, J. Colloid Interface Sci. 341 (1) (2010) 88–93.
[28] V. Nigro, F. Ripanti, R. Angelini, A. Sarra, M. Bertoldo, E. Buratti, P. Postorino, B. Ruzicka, Molecular mechanisms driving the microgels behaviour: a Raman spectroscopy and dynamic light scattering study, J. Mol. Liq. 284 (2019) 718–724.
[29] S. Franco, E. Buratti, V. Nigro, M. Bertoldo, B. Ruzicka, R. Angelini, Thermal behaviour of microgels composed of interpenetrating polymer networks of poly (n-isopropylacrylamide) and poly (acrylic acid): a calorimetric study, Polymers 14 (1) (2022) 115.
[30] V. Nigro, R. Angelini, B. Rosi, M. Bertoldo, E. Buratti, S. Casciardi, S. Sennato, B. Ruzicka, Study of network composition in interpenetrating polymer networks of poly(N isopropylacrylamide) microgels: the role of poly(acrylic acid), J. Colloid Interface Sci. 545 (2019) 210–219.
[31] S. Franco, E. Buratti, V. Nigro, E. Zaccarelli, B. Ruzicka, R. Angelini, Glass and jamming rheology in soft particles made of pnipam and polyacrylic acid, Int. J. Mol. Sci. 22 (8) (2021) 4032.
[32] V. Nigro, B. Ruzicka, B. Ruta, F. Zontone, M. Bertoldo, E. Buratti, R. Angelini, Relaxation dynamics, softness, and fragility of microgels with interpenetrated polymer networks, Macromolecules 53 (2020) 1596–1603.
[33] M.R. Islam, S. Xie, D. Huang, K. Smyth, M.J. Serpe, Poly (n-isopropylacrylamide) microgel-based optical devices for humidity sensing, Anal. Chim. Acta 898 (2015) 101–108.
[34] J. Liu, T. Shu, L. Su, X. Zhang, M.J. Serpe, Synthesis of poly (n-isopropylacrylamide)-co-(acrylic acid) microgel-entrapped cds quantum dots and their photocatalytic degradation of an organic dye, RSC Adv. 8 (30) (2018) 16850–16857.
[35] T. Brändel, L. Wiehemeier, T. Kottke, T. Hellweg, Microphase separation of smart double-responsive copolymer microgels studied by local fluorescence probes, Polymer 125 (2017) 110–116.
[36] Z.H. Farooqi, H.U. Khan, S.M. Shah, M. Siddiq, Stability of poly (n-isopropylacrylamide-co-acrylic acid) polymer microgels under various conditions of temperature, ph and salt concentration, Arab. J. Chem. 10 (3) (2017) 329–335.
[37] N. Seddiki, D. Aliouche, Synthesis, rheological behavior and swelling properties of copolymer hydrogels based on poly (n-isopropylacrylamide) with hydrophilic monomers, Bull. Chem. Soc. Ethiop. 27 (3) (2013) 447–457.
[38] S.B. Debord, L.A. Lyon, Influence of particle volume fraction on packing in responsive hydrogel colloidal crystals, J. Phys. Chem. B 107 (13) (2003) 2927–2932.
[39] X. Wang, Y. Li, G. Zhang, B. Wang, Study on the morphology and temperature-sensitivity of poly (n-isopropylacrylamide-co-acrylic acid) microgel by atomic force microscope, E3S Web Conf. 267 (2021) 02007, EDP Sciences.
[40] J.B. Thorne, G.J. Vine, M.J. Snowden, Microgel applications and commercial considerations, Colloid Polym. Sci. 289 (2011) 625–646.
[41] E.Y. Kozhunova, O.V. Vyshivannaya, I.R. Nasimova, "Smart" IPN microgels with different network structures: self-crosslinked vs conventionally crosslinked, Polymer 176 (2019) 127–134.
[42] R.H. Pelton, P. Chibante, Preparation of aqueous lattices with N-isopropylacrylamide, Colloids Surf. 20 (1986) 247–256.
[43] V. Nigro, R. Angelini, M. Bertoldo, F. Bruni, M. Ricci, B. Ruzicka, Dynamical behavior of microgels of interpenetrated polymer networks, Soft Matter 13 (2017) 5185–5193.
[44] F. Capitani, S. Koval, R. Fittipaldi, S. Caramazza, E. Paris, W. Mohamed, J. Lorenzana, A. Nucara, L. Rocco, A. Vecchione, et al., Raman phonon spectrum of the Dzyaloshinskii-Moriya helimagnet ba 2 cuge 2 o 7, Phys. Rev. B 91 (21) (2015) 214308.
[45] C.W. Makosko, Rheology: Principles, Measurements and Applications, Vch Pub, 1994.
[46] H. Senff, W. Richtering, Influence of cross-link density on rheological properties of temperature-sensitive microgel suspensions, Colloid Polym. Sci. 278 (2000) 830–840.

[47] M.M. Cross, Rheology of non-Newtonian fluids: a new flow equation for pseudoplastic systems, J. Colloid Sci. 20 (2007) 417–437.
[48] C. Pellet, M. Cloitre, The glass and jamming transitions of soft polyelectrolyte microgel suspensions, Soft Matter 12 (2016) 3710–3720.
[49] A. Kardos, T. Gilányi, I. Varga, How small can poly (n-isopropylacrylamide) nanogels be prepared by controlling the size with surfactant?, J. Colloid Interface Sci. 557 (2019) 793–806.
[50] D. Schlattmann, M. Schönhoff, Interplay of the influence of crosslinker content and model drugs on the phase transition of thermoresponsive pnipam-bis microgels, Gels 8 (9) (2022) 571.
[51] T. Hoare, D. McLean, Kinetic prediction of functional group distributions in thermosensitive microgels, J. Phys. Chem. B 110 (41) (2006) 20327–20336.
[52] R. Elancheliyan, G. Del Monte, E. Chauveau, S. Sennato, E. Zaccarelli, D. Truzzolillo, Role of charge content in the two-step deswelling of poly (n-isopropylacrylamide)-based microgels, Macromolecules 55 (17) (2022) 7526–7539.
[53] L. Tavagnacco, E. Zaccarelli, E. Chiessi, On the molecular origin of the cooperative coil-to-globule transition of poly (n-isopropylacrylamide) in water, Phys. Chem. Chem. Phys. 20 (15) (2018) 9997–10010.
[54] M. Berberan-Santos, E. Bodunov, B. Valeur, Mathematical functions for the analysis of luminescence decays with underlying distributions: 2. Becquerel (compressed hyperbola) and related decay functions, Chem. Phys. 317 (1) (2005) 57–62.
[55] Z. Ahmed, E.A. Gooding, K.V. Pimenov, L. Wang, S.A. Asher, Uv resonance Raman determination of molecular mechanism of poly (n-isopropylacrylamide) volume phase transition, J. Phys. Chem. B 113 (13) (2009) 4248–4256.
[56] J. Dybal, M. Trchová, P. Schmidt, The role of water in structural changes of poly (n-isopropylacrylamide) and poly (n-isopropylmethacrylamide) studied by ftir, Raman spectroscopy and quantum chemical calculations, Vib. Spectrosc. 51 (1) (2009) 44–51.
[57] P. Schmidt, J. Dybal, M. Trchová, Investigations of the hydrophobic and hydrophilic interactions in polymer–water systems by atr ftir and Raman spectroscopy, Vib. Spectrosc. 42 (2) (2006) 278–283.
[58] A.M. Howe, S. Desrousseaux, L.S. Lunel, J. Tavacoli, A.F.R.H.N. Yow, Anomalous viscosity jump during the volume phase transition of poly(N-isopropylacrylamide) particles, Adv. Colloid Interface Sci. 148 (148) (2008) 124–131.